SciMedCentral

Journal of Urology and Research

Research Article

Transient Thermal Lens Simulation of Ho:YAG Laser

Yang-Te T Fan and Jian J Zhang*

Boston Scientific Corporation, Marlborough, USA

*Corresponding author

Jian J Zhang, Boston Scientific Corporation, Marlborough, MA 01752, USA

Submitted: 29 November 2022

Accepted: 15 December 2022

Published: 16 December 2022

ISSN: 2379-951X

Keywords

- Laser Lithotripsy
- Ho: YAG
- Transient Thermal Behavior
- Preheating
- Temperature Profile
- Thermal Lens
- Laser Cavity Stable Zone

Abstract

The Ho:YAG laser has been the favored lithotripter for the treatment of urinary calculi since shortly after its introduction in the 1990s, because it can fragment all calculus compositions and produces less calculus migration (retropulsion) during treatment than the short-pulsed lasers [Marks AJ et al., World Journal of Urology. 2007; 25(3): 227]. Although the lamp-pumped Ho:YAG laser has been commercialized for ureteroscopic laser lithotripsy (URSL) for almost 25 years, the transient thermal behavior of the lamp-pumped laser rod is difficult to estimate. The objective of this study is to simulate the transient thermal behavior of the lamp-pumped laser rod from preheating to laser operation. The temperature profile inside the laser rod is transformed into an equivalent thermal lens, and from the time interval of the variation of the thermal lens between lasing threshold and the maximum value of stable region, we can estimate the level of the laser output. The simulation tool used for this study is the Ansys Fluent, and the transient thermal behavior of the lamp-pumped laser rod from preheating to laser operation was reported. Optimization of the pumping pulse for the desired laser output pulse is for a future study.

INTRODUCTION

The retrospective study in [1], revealed superior stone-free rate (SFR) results for renal stones < 1.5 cm by ureteroscopic laser lithotripsy (URS) compared with SWL. The Ho:YAG laser has been the favored lithotripter for the treatment of urinary calcului since shortly after its introduction in the 1990s [2-3], because it can fragment all calculus compositions and produces less calculus migration (retropulsion) during treatment than the short-pulsed lasers [4]. Although the lamp-pumped Ho:YAG laser has been commercialized for URS for almost 25 years, the lamp-pumped laser rod's transient thermal lens behavior with preheating pulses has not been reported. Modern laser design usually includes some negative lens to compensate the thermal lens to achieve higher performance (higher power with higher brightness). Therefore, the laser threshold will require a certain level of thermal lens, and preheating is a necessity to begin lasing.

The objective of this study is to simulate the transient thermal lens behavior of the lamp-pumped laser rod from preheating to laser operation. The temperature profile inside the laser rod is transformed into an equivalent thermal lens, and from the time interval of the variation of the thermal lens between lasing threshold and the maximum value of the stable region, we can estimate the level of the laser output. The simulation tool used for this study is the Ansys Fluent, and the transient thermal behavior of the lamp-pumped laser rod from preheating to laser operation was reported. Optimization of the pumping pulse for the desired laser output pulse is for a future study.

SIMULATION METHOD

Depending on the cavity design (parameters like resonator cavity arm length, mirror curvatures, intracavity optics, gain medium thermal lens, etc.), the laser resonator cavity has two stability zones in which stable cavity modes exist that warrant laser output, as illustrated in Figure 1 [5,6]. Since the thermal lens (a variable cavity parameter) governs the stability of the laser resonator, and the thermal lens depends on the input power, we need to characterize: 1) the input power; and 2) the relationship between thermal profile and thermal lens (Figure 1).

The input conditions

The input power is the heat generated inside the rod because of pumping energy from the flash lamp. The pump source, Xenon flash lamp, has an electrical to light efficiency of ~50% [7], its

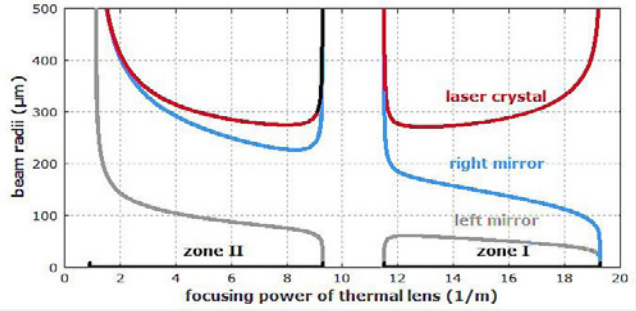

Figure 1 Stability diagram of a laser resonator cavity.

spectrum covers 200-1000 nm. The laser crystal is CTH:YAG, and its absorption band has a few peaks in the visible spectrum [8-9]. Fig. 2 shows input conditions for the Xenon lamp emission spectrum [7], and CTH:YAG Absorption Coefficient [8,9] (Figure 2).

The overall conversion efficiencies of pulsed lamp light to the laser crystal's absorbed energy can be in the η = 50–80% region [10]. Since the water is transparent to the visible spectrum [11], the lamp radiation loss in the coolant is negligible.

The relationship between thermal profile and thermal lens

With a simplified model, Steady-State Condition, we consider the case where the heat generated within the laser rod by pump-light absorption is removed by a coolant flowing along the cylindrical rod surface [6]. With the assumption of uniform internal heat generation and cooling along the cylindrical surface of an infinitely long rod, the heat flow is strictly radial, no end effects, and the small variation of coolant temperature in the axial direction can be neglected. The radial temperature distribution in a cylindrical rod is obtained from the one-dimensional heat conduction equations:

$$\frac{d^2T}{dr^2}+\left(\frac{1}{r}\right)\left(\frac{dT}{dr}\right)+\frac{Q}{K}=0 \quad (1)$$

$$T(r)=T(r_0)+\left(\frac{Q}{4K}\right)\left(r_0^{\,2}-r^2\right) \quad (2)$$

$$Q=\frac{P_{heat}}{\pi r_0^{\,2} l} \quad (3)$$

$$\Delta T=T(0)-T(r_0)=\frac{P_{heat}}{4\pi K l} \quad (4)$$

where T is the temperature in the laser rod, r is the rod radius ranging from 0 to r_0, l is the length of the rod, K is the thermal conductivity, Q is the heat at a rate per unit volume, P_{heat} is uniformly 12 generated heating power or the dissipated thermal power.

Assuming the temperature profile is approximately parabolic, and the laser gain medium is isotropic in which there are a uniform pump intensity and a purely radial heat flow, we then have 16 a thermal lens with the dioptric power (inverse focal length)

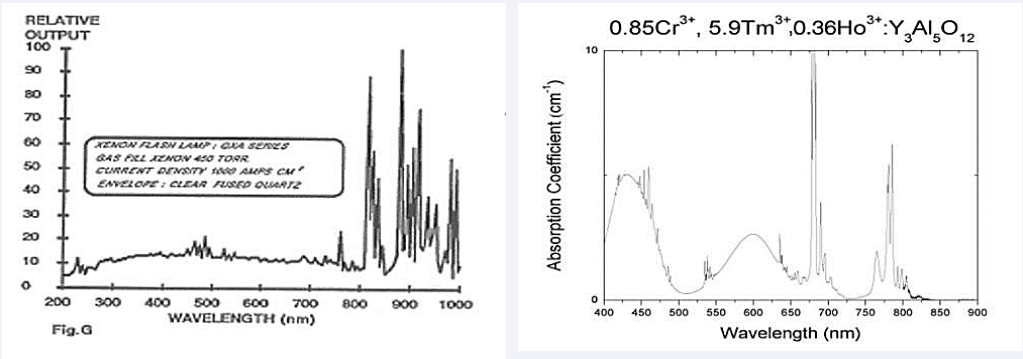

Figure 2 Input conditions: (a) the Xenon lamp emission spectrum; (b) CTH:YAG Absorption Coefficient.

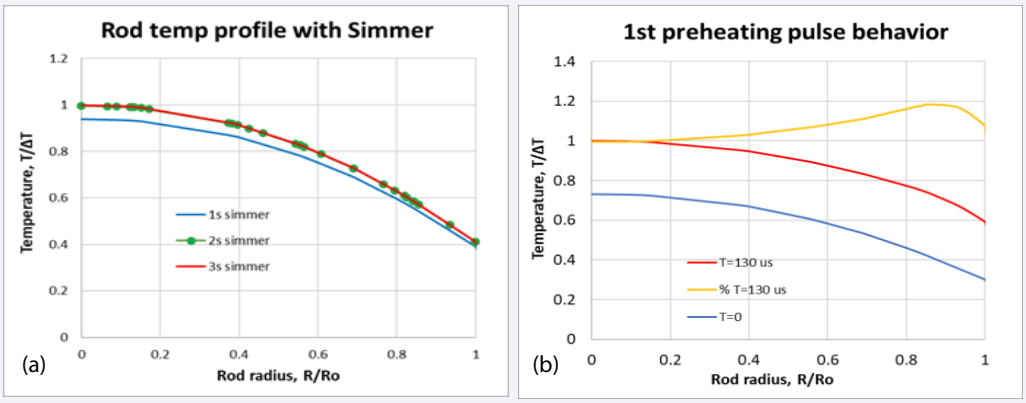

Figure 3 Temperature profile of the simulation result: (a) Rod temperature profile at 1s, 2s, 3s of simmer; (b) Rod temperature profile after the 1st preheating pulse.

$$f^{-1} = \frac{dn/dT}{2KA} P_{heat} \quad (5)$$

where f is the thermal lens, n is the refractive index under conditions of constant strain, A is the pumped area. From Equations (4) and (5), we got

$$\Delta T = 1.9 f^{-1} \quad (6)$$

The simulation tool

The ANSYS Fluent is a powerful Computational Fluid Dynamics (CFD) tool for flow and thermal simulation. The simulation models and boundary condition settings can be applied to the most complicated conditions. It provides an accurate simulation of the laser pumping chamber (3D model of the rod, flow tube, cooling flow and pumping radiation, etc.) with Task-based and streamlined workflows. The software tool provides the output of temperature contours along the laser rod's axial and radial sections.

SIMULATION RESULTS

Single preheating pulse case

In our previous publication [12], we demonstrated the simulation of a single preheating pulse: pulse width ~130 μs, heating energy ~6.32 J (~48.6 kW heating power). Moreover, the average temperature rise of the simulation result is 1.38 ºC, which matches well with the theoretical estimation of 1.39 ºC.

In an actual laser device, there is a constant simmer current running to the flash lamp to reduce its impedance to a constant value, and therefore an increase of the peak current through the flash lamp is observed, which improves the flash-lamp efficiency. With a typical simmer current of 100-200 mA, the laser rod with 18.2 ºC, 1.2 GPM coolant flow will reach temperature equilibrium after 3 seconds (three times that of the thermal time constant ~ 1 s of the rod), as shown in Figure 3. And from the simulation result of the 1st preheating pulse in Figure 3, the relative temperature rise after the 1st pre-pulse has a ~ 20% max temp rise near the rod surface (matches very well with the theoretical estimation [6]).(Figure 3)

Multiple preheating pulse case

The multiple preheating pulse case is multiple single preheating pulses with a certain repetition rate. If we use the same single preheating pulse: at a repetition rate of 50 Hz for 0.25 s, there will be 12 preheating pulses at an interval of 20 ms. Again, in our previous publications [12-13], we reported the shape of the temperature profile after the preheating pulses matched very well with theoretical estimation in ref [6]. Figure 4 is the temperature profile of the simulation result with simmer-on at all the time (Figure 4).

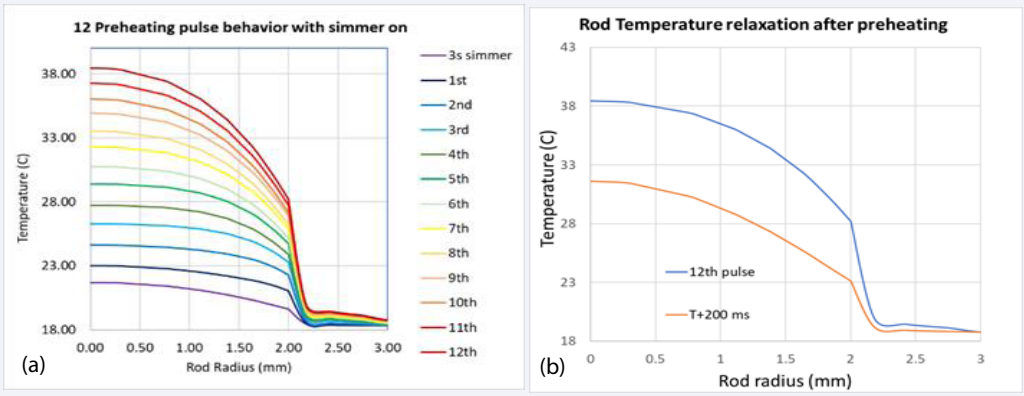

Figure 4 Temperature profile of the simulation result of 12 preheating pulses: (a) Simulation result right after each preheating pulse; (b) Rod temperature relaxation after the preheating pulses.

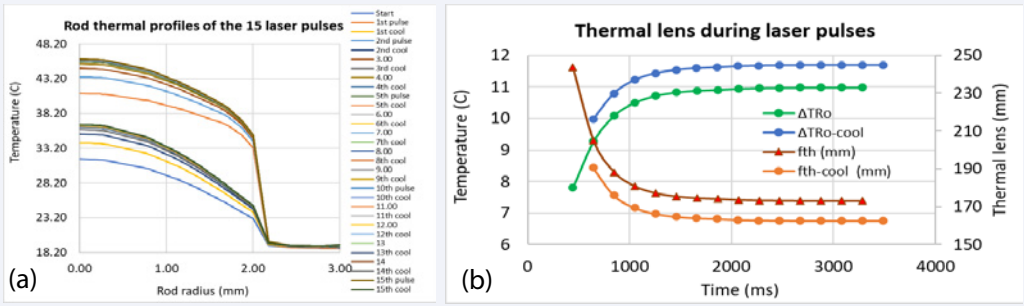

Figure 5 Temperature profile and thermal lens of the simulation result of 15 laser pulses: (a) Temperature profile of each laser pulse; (b) Thermal lens before and after the laser pulses.

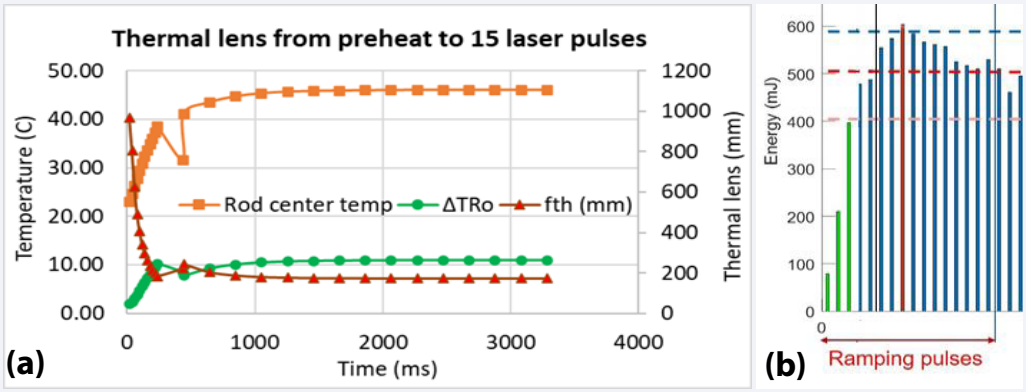

Figure 6 Simulation result and experimental measurement: (a) Thermal lens simulation from preheating; (b) Laser pulse ramp-up test result by energy meter.

Thermal lens

With Equation (6) and the temperature difference between the rod center and the edge, we can find the thermal lens during laser pulses, as shown in Figure 5. At lasing state, the temperature profile and thermal lens reach two stable states (or oscillate between two states). The conditions with the label "cool" mean ~3 ms before the laser pulse injection, and the conditions without the "cool" label mean right after the laser pulse injection. From Fig. 5 (b), the temperature difference between the rod center and the edge is bigger before (ΔTRo-cool) the laser pulse than after (ΔTRo) the laser pulse because the side-pumped pulse of the laser increased the edge temperature, which reduced the temperature difference. Moreover, the thermal lens is reciprocally related to the temperature difference; therefore, the thermal lens is stronger (shorter) before (fth-cool) lasing. The laser pulse reduces the temperature drop because of the stronger absorption near the surface of the rod by side pumping laser design (Figure 5).

Figure 6 is the thermal lens simulation from preheating and the laser pulse ramp-up test result by energy meter. From the thermal lens simulation, we can see the preheating buildup of the thermal lens preparing the laser rod for lasing (even with a dip during the 200 ms cool down system preparation time). The thermal lens ramps up during laser pulses. It takes 4-8 pulses to reach thermal equilibrium. The laser test results in Figure 6 (b) is a pulse energy ramp-up graph. Since this prototype laser has four laser cavities, each consecutive four pulses of Figure 6 (b) correspond to one data point in Figure 6 (a). It seems that the second laser pulse (in (a)) of each cavity (the 5-8 pulses in (b)) reaches the peak energy output level, and the 4th laser pulse (in (a)) of each cavity (the 1316 pulses in (b)) reaches the target energy output level (Figure 6).

DISCUSSION

There are a few limitations of this simulation. The first limitation is about Equation (4). With the assumption of uniform internal heat generation (Pheat) and cooling along the cylindrical surface of an infinitely long rod, the heat flow is strictly radial, with no end effects, and the small variation of coolant temperature along axial direction can be neglected. The second limitation is about Equation (5), which suggests that the rod's temperature profile is parabolic and that the experimental data of dn/dT is not reliable.

Even with the limitations mentioned above, the preheating pulses' simulation results match the theoretical estimation very well. When adding the simmer current (~150mA), the relative temperature rise after the 1st pre-pulse has a ~ 20% maximum temperature rise near the rod surface, which matches very well with the theoretical estimation [6]. After the 12 preheating pulses and 200ms relaxation, the simmer current helps increase the temperature difference from ~2 ºC to reach ~8.5 ºC, which is equivalent to a thermal lens of ~224 mm.

At lasing state, the temperature profile and thermal lens oscillate between two states. Also, the temperature difference between the rod center and the edge is bigger before (ΔTRo-cool) the laser pulse than after (ΔTRo), and the thermal lens is stronger (shorter) before (fth-cool) lasing because the laser pulse reduces the temperature drop as a result of the stronger absorption near the surface of the rod by side pumping laser design. The simulation also shows that it takes each cavity ~4 pulses to reach thermal equilibrium (ramp-up) during laser pulses, and it matches the laser test result of 16-pulse energy ramp-up behavior (four cavities total).

CONCLUSION

The simulation results of preheating pulses with simmer current by Ansys Fluent match the theoretical estimation very well. The transient thermal lens (fth) demonstrated that preheating pulses can help the laser reach the stable state faster and that at the lasing state, fth reaches two stable states. Additionally, fth is stronger before each laser pulse than after. Further validation and optimization of the laser output pulse and preheating pulse are for future study.

DISCLAIMERS

REFERENCES

1. Cone EB, Eisner BH, Ursiny M, Pareek G. Cost-effectiveness comparison of renal calculi treated with Ureteroscopic laser lithotripsy versus shockwave lithotripsy. J Endourol. 2014; 28: 639–643.
2. G Watson, N Smith. Comparison of the pulsed dye and holmium lasers for stone fragmentation: *in-vitro* studies and clinical experience. Proc SPIE. 1993; 1879: 139–142.
3. J Sayer, DE Johnson, RE Price. Cromeens DM. Endoscopic laser fragmentation of ureteral calculi using the holmium:YAG. Proc SPIE. 1993; 1879: 143–148.
4. Marks AJ, Teichman JM. Lasers in clinical urology: state of the art and new horizons. World J Urol. 2007; 25: 227–233.
5. Magni V. Multielement stable resonators containing a variable lens. JOSA A. 1987; 4: 1962-1969.
6. Koechner W. Solid-State Laser Engineering. Sixth Revised and Updated Edition. 2006.
7. Eg&G. High Performance Flash and Arc Lamps. PerkinElmer Optoelectronics.
8. Antipenko BM, Berezin YD, Buchenkov VA, Zhurba VM, Kiseleva TI, Lazo VV, et al. Pulse-periodic holmium laser for medical applications. Sov J Quantum Electron. 1989; 19: 1509.
9. Kaminskii AA. Crystalline Lasers: Physical Processes and Operating Schemes. CRC Press, New York. 1996.
10. The lamp book. The Heraeus Noblelight technical reference book for arc and flash lamps. 11.
11. Chaplin M. Water Structure and Science. Transparency of Water in the Visible Range.
12. Fan YT, Zhang JJ. Transient Thermal Simulation of Lamp-Pumped Ho-YAG laser. Proc SPIE. 2021; 11619.
13. Ibey, Bennett L. Optical Interactions with Tissue and Cells XXXIII; and Advanced Photonics in Urology. Proc SPIE. 2022; 1: 1-128.